

Characterization of Salt Bridges to Lysines in the Protein G B1 Domain

Jennifer H. Tomlinson,[†] Saif Ullah,[‡] Poul Erik Hansen,[‡] and Mike P. Williamson^{*†}

Department of Molecular Biology and Biotechnology, University of Sheffield, Firth Court, Western Bank, Sheffield, S10 2TN U.K., and Department of Science, Systems and Models, Roskilde University, DK-4000 Roskilde, Denmark

Received October 20, 2008; E-mail: m.williamson@sheffield.ac.uk

Abstract: NMR investigations have been carried out on the B1 domain of protein G. This protein has six lysine residues, of which three are consistently found to form surface-exposed salt bridges in crystal structures, while the other three are not. The $N\zeta$ and $H\zeta$ chemical shifts of all six lysines are similar and are not affected significantly by pH titration of the carboxylate groups in the protein, except for a relatively small titration of K39 $N\zeta$. Deuterium isotope effects on nitrogen and proton are of the size expected for a simple hydrated amine (a result supported by density functional theory calculations), and also do not titrate with the carboxylates. The line shapes of the J -coupled ^{15}N signals suggest rapid internal reorientation of all NH_3^+ groups. pK_a values have been measured for all charged side chains except Glu50 and do not show the perturbations expected for salt bridge formation, except that E35 has a Hill coefficient of 0.84. The main differential effect seen is that the lysines that are involved in salt bridges in the crystal display faster exchange of the amine protons with the solvent, an effect attributed to general base catalysis by the carboxylates. This explanation is supported by varying buffer composition, which demonstrates reduced electrostatic shielding at low concentration. In conclusion, the study demonstrates that the six surface-exposed lysines in protein G are not involved in significant salt bridge interactions, even though such interactions are found consistently in crystal structures. However, the intrahelical E35–K39 ($i,i+4$) interaction is partially present.

Introduction

A salt bridge is a noncovalent bond between two oppositely charged residues that experience an electrostatic attraction.^{1–4} These salt bridges can be considered as special forms of hydrogen bonds.¹ Although buried salt bridges appear to have an important role in protein structure and stability,^{5–7} the role of solvent-exposed salt bridges in protein structure is less clear, with some studies finding them to be stabilizing,⁸ some destabilizing,⁹ and some insignificant.^{7,10,11} One study found that the strength of a salt bridge was inversely correlated to the degree of solvent exposure.⁷ The coupling free energy of

exposed salt bridges has generally been found to be weaker than that of buried salt bridges, but some studies suggest that they contribute to protein stability, and in particular it has been suggested that networks of salt bridges on the surface of proteins from thermophiles increase the thermostability of the protein.^{12,13} Differences in the influence of salt concentration on stability in the presence and in the absence of exposed salt bridges also suggest that exposed salt bridges have a role in stability.⁷ In crystal structures of proteins, solvent-exposed salt bridges are often seen, but it is far from clear whether such interactions are really stable in solution, where the entropic cost of restraining the two charged species together is similar in energy to the enthalpic benefit of a solvated charge–charge interaction.¹⁴ The significance of exposed salt bridges, therefore, remains uncertain.

The presence of salt bridges has been studied experimentally in two main ways, neither of which is ideal.^{1,8} The first is by mutating potential residues involved^{6,7,15,16} and measuring changes to the protein, usually in protein stability. The difficulty with this approach is that such mutations can have additional

[†] University of Sheffield.

[‡] Roskilde University.

- (1) Bosshard, H. R.; Marti, D. N.; Jelesarov, I. *J. Mol. Recognit.* **2004**, *17*, 1–16.
- (2) Horovitz, A.; Serrano, L.; Avron, B.; Bycroft, M.; Fersht, A. R. *J. Mol. Biol.* **1990**, *216*, 1031–1044.
- (3) Sarakatsannis, J. N.; Duan, Y. *Proteins: Struct., Funct. Bioinf.* **2005**, *60*, 732–739.
- (4) Barlow, D. J.; Thornton, J. M. *J. Mol. Biol.* **1983**, *168*, 867–885.
- (5) Dong, F.; Zhou, H. X. *Biophys. J.* **2002**, *83*, 1341–1347.
- (6) Tissot, A. C.; Vuilleumier, S.; Fersht, A. R. *Biochemistry* **1996**, *35*, 6786–6794.
- (7) Takano, K.; Tsuchimori, K.; Yamagata, Y.; Yutani, K. *Biochemistry* **2000**, *39*, 12375–12381.
- (8) Vijayakumar, M.; Zhou, H. X. *J. Phys. Chem. B* **2001**, *105*, 7334–7340.
- (9) Sindelar, C. V.; Hendsch, Z. S.; Tidor, B. *Protein Sci.* **1998**, *7*, 1898–1914.
- (10) Šali, D.; Bycroft, M.; Fersht, A. R. *J. Mol. Biol.* **1991**, *220*, 779–788.
- (11) Strop, P.; Mayo, S. L. *Biochemistry* **2000**, *39*, 1251–1255.

- (12) Merz, T.; Wetzel, S. K.; Firbank, S.; Plückthun, A.; Grütter, M. G.; Mittl, P. R. E. *J. Mol. Biol.* **2008**, *376*, 232–240.
- (13) Kobayashi, T.; Kageyama, Y.; Sumitomo, N.; Saeki, K.; Shirai, T.; Ito, S. *World J. Microbiol. Biotechnol* **2005**, *21*, 961–967.
- (14) Sun, D. P.; Sauer, U.; Nicholson, H.; Matthews, B. W. *Biochemistry* **1991**, *30*, 7142–7153.
- (15) Luisi, D. L.; Snow, C. D.; Lin, J. J.; Hendsch, Z. S.; Tidor, B.; Raleigh, D. P. *Biochemistry* **2003**, *42*, 7050–7060.
- (16) de Prat Gay, G.; Johnson, C. M.; Fersht, A. R. *Protein Eng.* **1994**, *7*, 103–108.

effects, causing altered nonelectrostatic interactions and possibly conformational changes that would also have effects on the stability of the protein.^{1,15} This problem is partly solved by using double mutant cycles. However, the coupling energies determined by such studies can sometimes differ, depending on the mutants chosen,¹⁵ and most reported double mutant cycles use only one set of mutants. Changes in the structure or interactions in the unfolded state are also not accounted for in double mutant cycles.¹⁵

The second experimental approach is to measure changes in the pK_a of salt-bridging residues upon folding.^{17,18} Problems with this method include potential interactions in the unfolded state, plus general electrostatic effects in the folded state.¹ The pK_a of a carboxylate side chain involved in a salt bridge will be lowered because the salt bridge interaction stabilizes the negative charge, while that of a lysine will be increased because the positive charge is stabilized by the salt bridge.¹⁹ Similarly, increases in the pK_a of carboxylates involved in salt bridges in response to substitution of lysines with neutral residues have been used to gauge the strength of salt bridges.^{19,20}

Salt bridges involving lysines should also be observable via their effect on the deuterium isotope effect (the chemical shift change of ¹⁵N or ¹H arising from substitution of NH by ND), which is expected to be different for hydrogen-bonded systems. Both experiments^{21–24} and calculations^{23,25} show that the isotope effect on both N and H in ammonium compounds varies with solvation and counterions, the effect varying with the hydrogen-bonding distance and therefore the strength of the hydrogen bond. Deuterium isotope effects can thus be used to characterize solvation as well as to tell about the nature and distance to counterions.^{23,25,26}

The 56-residue B1 domain of streptococcal protein G (referred to as protein G for the remainder of this report) binds to IgG and is thought to be important in avoidance of the host immune response. Both crystal and NMR structures have been determined,^{27,28} and protein G remains folded over a wide pH and temperature range. In most of the available crystal structures, three of the six lysine residues in protein G form salt bridges with carboxylate side chains, all of which are solvent-exposed. The remaining three lysines are solvent-exposed but do not form salt bridges. This allows comparisons to be made between lysines involved in exposed salt bridges and those that form no salt bridges.

We demonstrate that the main difference observed between lysine NH_3^+ groups involved in exposed salt bridges and those that form no salt bridge is an increased exchange rate seen for salt bridged residues, probably due to general base catalysis of exchange by the carboxylate side chain. Our data provide no

evidence of salt bridges in solution for two of the three lysines expected to take part in salt bridges (in 50 mM phosphate) and limited evidence for the third, in contrast to studies on buried salt bridges,^{29,30} suggesting that solvent-exposed salt bridges are not significant interactions in solution.

Materials and Methods

Protein Expression and Purification and Sample Preparation. Protein G B1 domain was expressed as a His-tagged construct with the sequence MH₆AMD preceding the normal N-terminal sequence from a gene inserted into a pET-15b vector. The protein was expressed in *Escherichia coli* BL21 (DE3) pLysS cells grown in M9 minimal medium containing 1.5 g/L ¹³C-glucose, 1 g/L ¹⁵N-ammonium sulfate, 34 μg/mL chloramphenicol, and 50 μg/mL carbenicillin. Expression was induced by 1 mM IPTG when an OD_{600nm} of 0.6 was reached, and cultures were incubated overnight at 25 °C. Cells were harvested by centrifugation and lysed by freeze–thaw. The protein was purified using a nickel affinity column (His-select nickel affinity gel, Sigma-Aldrich) followed by gel filtration in 50 mM potassium phosphate buffer plus 150 mM NaCl and 1 mM sodium azide, pH 6.0. Buffer exchange and protein concentration was carried out in vivaspin centrifugal concentrators (Sartorius).

Samples for pK_a measurements were produced in a buffer containing 33 mM deuterated sodium acetate, 33 mM sodium phosphate, and 33 mM boric acid at 1 mM protein G for H(C)CO and HC(CO) spectra and 2 mM protein G for H₂CN spectra. pH change was done by dialysis, implying that salt concentrations remained approximately the same throughout the titrations. All other samples were produced at 0.4 mM protein G in 50 mM potassium phosphate buffer. All samples were produced in 90% H₂O/10% D₂O (except where noted otherwise) and contained 1 mM sodium azide. For analysis of the coupled methyl line shape the sample was prepared in 100% H₂O with a capillary tube of D₂O inside the sample. Samples for H₂CN spectra were degassed by bubbling nitrogen through the sample, and the sample tube was filled with nitrogen to prevent carbon dioxide dissolving in the sample and reducing the pH.

NMR Experiments and Data Processing. All spectra were acquired on a 600 MHz Bruker DRX-600 spectrometer fitted with a cryoprobe. Spectra were processed using Felix (Accelrys Inc., San Diego, CA), and data were analyzed using home-written scripts running under Linux.

HISQC spectra to measure the NH_3^+ , NH_2D^+ , and NHD_2^+ chemical shifts were acquired as described, using deuterium decoupling in all cases.²⁹ All spectra were acquired at 278 K (calibrated using methanol). Spectra were acquired in 40% D₂O at pH 5.45, 4.95, 4.47, and 3.46 and in 100% H₂O with a capillary of D₂O in the sample at pH 5.59 with and without decoupling during t_1 . Additional HISQC spectra were collected at pH 3.99 in 100% H₂O with nitrogen spectral widths ranging from 4 to 25 ppm.

Assignment of the lysine NH_3^+ groups was carried out through comparison of CCH-TOCSY, H₃NCECD, and (H)CCENH₃ spectra, acquired as described²⁹ at 278 K using a 0.4 mM sample of protein G at pH 5.51 in 95% D₂O. Two-dimensional H₂CN spectra for lysine pK_a determination were acquired using the pulse program described.³¹ Spectra were acquired at 303 K with a nitrogen spectral width of 15 ppm and a nitrogen offset of 27.5 ppm. Data were collected every 0.5 pH unit from pH 8.0 to 11.0. Sample pH was measured before and after data collection, and an average of the two measurements was taken as the sample pH. The pH did not vary by more than 0.1 pH unit except for the pH 8.5 sample which

- (17) Anderson, D. E.; Becktel, W. J.; Dahlquist, F. W. *Biochemistry* **1990**, *29*, 2403–2408.
- (18) Marti, D. N.; Bosshard, H. R. *J. Mol. Biol.* **2003**, *330*, 621–637.
- (19) Sundd, M.; Iverson, N.; Ibarra-Molero, B.; Sanchez-Ruiz, J. M.; Robertson, A. D. *Biochemistry* **2002**, *41*, 7586–7596.
- (20) Sundd, M.; Robertson, A. D. *J. Mol. Biol.* **2003**, *332*, 927–936.
- (21) Lyčka, A.; Hansen, P. E. *Magn. Reson. Chem.* **1985**, *23*, 973–976.
- (22) Hansen, P. E.; Lyčka, A. *Acta Chem. Scand.* **1989**, *43*, 222–232.
- (23) Hansen, P. E.; Hansen, A. E.; Lyčka, A.; Buvári-Barcza, A. *Acta Chem. Scand.* **1993**, *47*, 777–788.
- (24) Sanders, J. K. M.; Hunter, B. K.; Jameson, C. J.; Romeo, G. *Chem. Phys. Lett.* **1988**, *143*, 471–476.
- (25) Munch, M.; Hansen, A. E.; Hansen, P. E.; Bouman, T. D. *Acta Chem. Scand.* **1992**, *46*, 1065–1071.
- (26) Hansen, P. E. *Magn. Reson. Chem.* **2000**, *38*, 1–10.
- (27) Gronenborn, A. M.; Filpula, D. R.; Essig, N. Z.; Achari, A.; Whitlow, M.; Wingfield, P. T.; Clore, G. M. *Science* **1991**, *253*, 657–661.
- (28) Gallagher, T.; Alexander, P.; Bryan, P.; Gilliland, G. L. *Biochemistry* **1994**, *33*, 4721–4729.

- (29) Iwahara, J.; Jung, Y. S.; Clore, G. M. *J. Am. Chem. Soc.* **2007**, *129*, 2971–2980.
- (30) Poon, D. K. Y.; Schubert, M.; Au, J.; Okon, M.; Withers, S. G.; McIntosh, L. P. *J. Am. Chem. Soc.* **2006**, *128*, 15388–15389.
- (31) André, I.; Linse, S.; Mulder, F. A. A. *J. Am. Chem. Soc.* **2007**, *129*, 15805–15813.

decreased by 0.2 pH unit over the course of the experiment. Protein was lost during buffer exchange between some samples, so subsequent experiments were carried out with greater numbers of scans to compensate for the reduction in protein concentration.

H(C)CO and HC(CO) spectra for measurement of glutamate and aspartate pK_a values were based on the Bruker HCACO pulse sequence with offsets altered to fit to the $C\beta/C\gamma$ shifts. Signal assignments were based on chemical shift assignments for this construct published previously.³²

pK_a Determination. Chemical shift changes with pH were fitted to the following equations describing dependence on one³³ or two³⁴ pK_a s, or one pK_a and a Hill coefficient different from unity:¹⁹

$$\delta = \frac{\delta_{\text{acid}} + \delta_{\text{base}} 10^{(\text{pH}-pK_a)}}{1 + 10^{(\text{pH}-pK_a)}} \quad (1)$$

$$\delta = \frac{\delta_a 10^{-2\text{pH}} + \delta_b 10^{-(\text{pH}+pK_{a1})} + \delta_c 10^{-(pK_{a1}+pK_{a2})}}{10^{-2\text{pH}} + 10^{-(\text{pH}+pK_{a1})} + 10^{-(pK_{a1}+pK_{a2})}} \quad (2)$$

$$\delta = \frac{\delta_{\text{acid}} + \delta_{\text{base}} 10^{n(\text{pH}-pK_a)}}{1 + 10^{n(\text{pH}-pK_a)}} \quad (3)$$

pK_a s were determined by simultaneously fitting the changes in C' , $C\beta/\gamma$, and $H\beta/\gamma$ shift. Because the ^1H data in general fitted less well to these equations than the ^{13}C data, inclusion of ^1H data made differences of <0.01 pH unit to the fitted pK_a values. Fitting was carried out using a Levenberg–Marquardt least-squares routine. F tests were carried out to determine which equation gave the best fit to the data.

DFT Calculations. Calculations were performed by density functional theory using the Gaussian 03 program, a B3LYP function, and a 6-31G(d) basis set. Shift changes on deuteration were calculated using the formula³⁵

$$\langle\sigma\rangle - \langle\sigma^*\rangle = \sum_i \left(\frac{\partial\sigma}{\partial r_{i_e}} \right) [\langle\Delta r_i\rangle - \langle\Delta r_i^*\rangle] + \sum_{ij} \left(\frac{\partial^2\sigma}{\partial r_i \partial r_j} \right) [\langle\Delta r_i \Delta r_j\rangle - \langle\Delta r_i \Delta r_j^*\rangle] + \sum_{ij} \left(\frac{\partial\sigma}{\partial \alpha_{ij}} \right) [\langle\Delta \alpha_{ij}\rangle - \langle\Delta \alpha_{ij}^*\rangle] + \dots \quad (4)$$

where the asterisked value refers to the deuterated nitrogen and the nonasterisked value to the protonated nitrogen. Only the first term in this equation was used, which is adequate for calculating the change in shift on deuteration.²⁵ Deuteration was mimicked by assuming a shortening of the NH bond by 0.0045 Å. Only the first carbon of the side chain of lysine was included. The geometries found in the Ipga crystal structure were used as the starting point and allowed to relax before calculation.

Results

Measurement and Assignment of Lysine NH Signals. Lysine side chain NH signals were observed directly at 278 K using an HISQC experiment²⁹ which is a modification of the standard HSQC experiment that is designed to deal effectively with the rapid amino proton exchange which otherwise leads to drastic

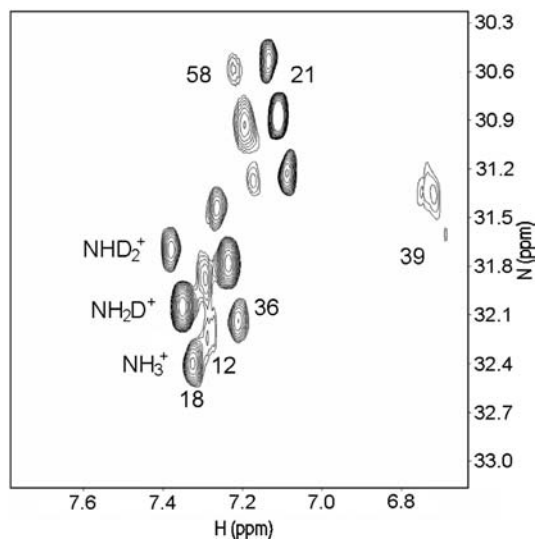


Figure 1. HISQC spectrum of lysine NH_3^+ groups at pH 5.45, 278 K in 40% D_2O . Three peaks are seen for K18, K21, K36, and K58, corresponding to NH_3^+ , NH_2D^+ , and NHD_2^+ groups (bottom right to top left, respectively; see labels on K18), while K12 shows only two peaks (the NHD_2^+ signal is lost in the negative wings of larger neighboring signals but is visible using different processing) and K39 has only a single broad signal due to chemical exchange (see text).

loss of signal intensity. Iwahara et al.²⁹ showed that NH_3^+ and NH_2D^+ groups give rise to signals with different chemical shift on both ^{15}N and ^1H , this difference being a deuterium isotope effect. We wished to study the size of this effect and therefore acquired spectra in 40% D_2O , in which the ratio of $\text{NH}_3:\text{NH}_2\text{D}:\text{NHD}_2$ is expected to be approximately 0.22:0.43:0.29, not accounting for relaxation effects. All six lysines were observed, although three were exchange broadened, and for five of the six, the expected isotope pattern was seen (Figure 1). Assignment of the HISQC peaks was carried out through the use of CCH-TOCSY, H_3NCECD , and (H)CCENH₃ spectra acquired as described (Supporting Information).²⁹ The assignment showed that the broad peaks are from K12, K39, and K58, which are the residues that consistently form salt bridges in crystal structures (Figure 2). The most rapidly exchanging lysine is K39, for which the exchange rate is fast enough to average the deuterium isotope effect, and must therefore be (slightly) greater than 21 Hz, followed by K12.

pH Dependence of Lysine NH_3^+ Chemical Shifts at Acidic pH. If the surface-exposed salt bridges are significant interactions, the chemical shifts of the lysine amines would be expected to change in response to titration of the carboxylate side chain. Therefore, HISQC spectra were acquired at pH 5.45, 4.95, 4.47, and 3.46 in 40% D_2O at 278 K, and the proton and nitrogen chemical shifts of the NH_3^+ peaks from these spectra were plotted against pH (Figure 3). None of the six lysines showed a significant change in proton chemical shift with pH, and only K21 and K39 showed a significant (>0.1 ppm) change in nitrogen chemical shift within the pH range 3.5–5.5. However,

(32) Tunnicliffe, R. B.; Waby, J. L.; Williams, R. J.; Williamson, M. P. *Structure* **2005**, *13*, 1677–1684.

(33) Khare, D.; Alexander, P.; Antosiewicz, J.; Bryan, P.; Gilson, M.; Orban, J. *Biochemistry* **1997**, *36*, 3580–3589.

(34) Joshi, M. D.; Sidhu, G.; Nielsen, J. E.; Brayer, G. D.; Withers, S. G.; McIntosh, L. P. *Biochemistry* **2001**, *40*, 10115–10139.

(35) Jameson, C. J. In *Isotopes in the physical and biomedical sciences*; Buncel, E., Jones, J. R., Eds.; Elsevier Science: Amsterdam, 1991; Vol. 2, p 1.

(36) Frericks Schmidt, H. L.; Sperling, L. J.; Gao, Y. G.; Wylie, B. J.; Boettcher, J. M.; Wilson, S. R.; Rienstra, C. A. *J. Phys. Chem. B* **2007**, *111*, 14362–14369.

(37) Nauli, S.; Kuhlman, B.; Le Trong, I.; Stenkamp, R. E.; Teller, D.; Baker, D. *Protein Sci.* **2002**, *11*, 2924–2931.

(38) Wunderlich, M.; Max, K. E. A.; Roske, Y.; Mueller, U.; Heinemann, U.; Schmid, F. X. *J. Mol. Biol.* **2007**, *373*, 775–784.

(39) Tugarinov, V.; Hwang, P. M.; Ollershaw, J. E.; Kay, L. E. *J. Am. Chem. Soc.* **2003**, *125*, 10420–10428.

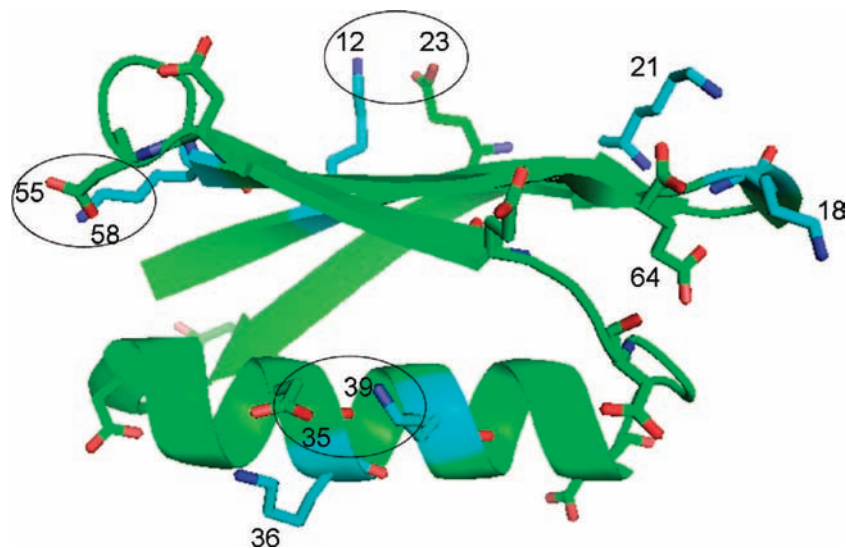


Figure 2. Crystal structure of protein G (PDB ID 1pga)²⁸ showing all lysine side chains in blue and all aspartate and glutamate side chains in green. The residues involved in salt bridges are circled. Similar interactions are found in other structures (PDB IDs 1pqb,²⁸ 2qmt,³⁶ 1mi0,³⁷ 2on8, and 2onq³⁸).

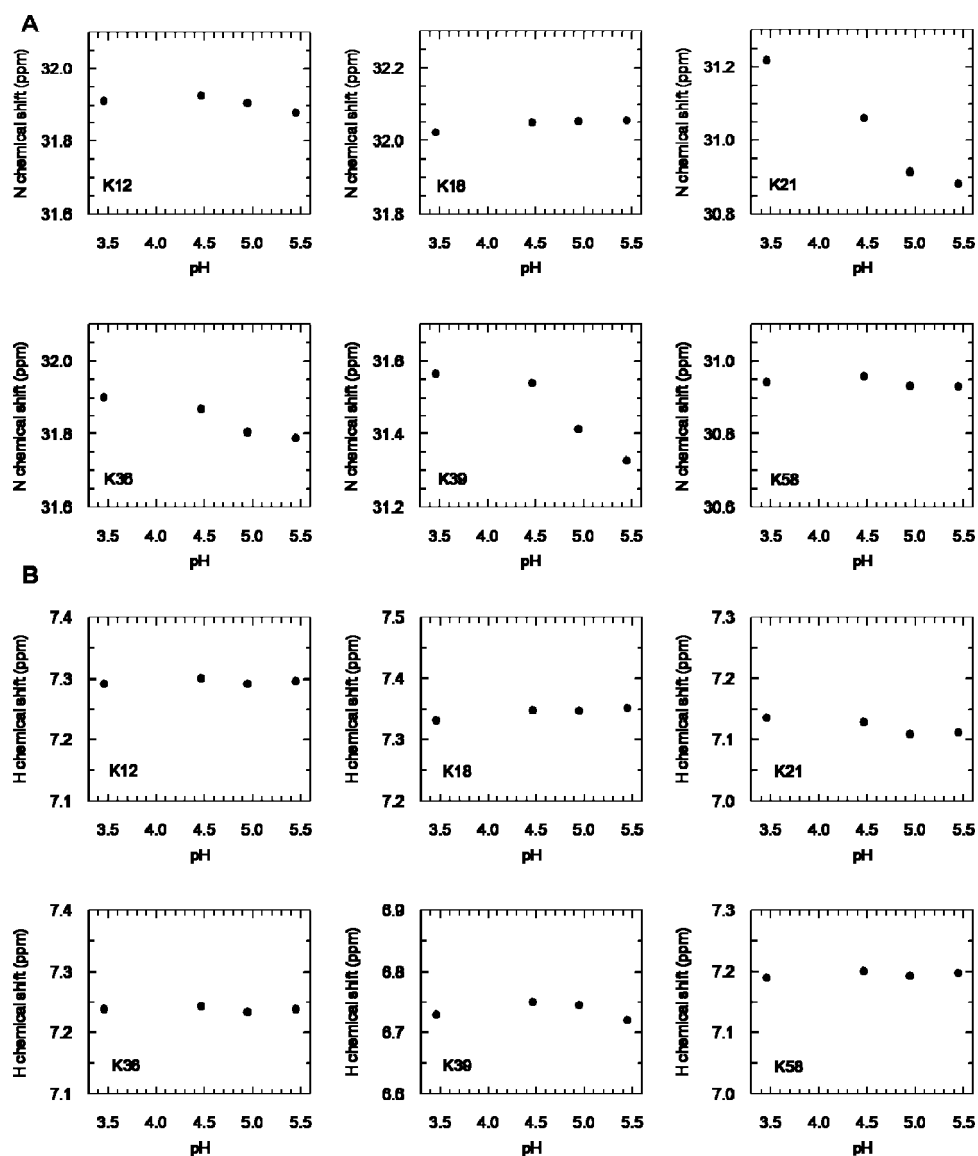


Figure 3. Changes in (A) nitrogen and (B) proton chemical shift with pH for lysine side chain NH_3 groups upon titration of carboxylate residues involved in salt bridges, taken from HISQC experiments.

Table 1. Deuterium Isotope Effects for Lysine ^{15}N and ^1H at pH 5.59, 50 mM Phosphate

residue	$^1\Delta\text{N(D)}$ (ppm)	$^2\Delta\text{H(D)}$ (ppm)
12	0.35	-0.027 ^b
18	0.35	-0.027
21	0.35	-0.023
36	0.35	-0.027
39	0.36 ^a	- ^c
58	0.35	-0.025

^a Less precisely determined because of exchange. ^b Estimated from values at lower pH because this signal is affected by exchange broadening (see text). ^c Not measurable because of exchange broadening.

Table 2. DFT Calculation of the ^{15}N Chemical Shift Change on Replacement of NH by ND

amino acid	H-bond	N...O distance (Å)	^{15}N shift change (ppm)		
			replacement of H1 ^a	replacement of H2	replacement of H3
lysine	none	—	0.464	0.400	0.468
K12	to E23	3.39	0.287	0.458	0.523
K39	to E35	3.03	0.196	0.502	0.513
K58	to D55	2.96	0.167	0.526	0.536

^a H1 is the proton that is intermediate between N and O.

K21 is not expected to form a salt bridge, and so the chemical shift of this residue is not expected to change with pH: we are unable to explain why this signal should change with pH. K39 is expected to form a salt bridge to E35, which has a pK_a of around 4.6 (see Table 3, below). The data in Figure 3 do not allow an accurate estimate of the observed change in nitrogen chemical shift with pH for K39, and it is possible that it does titrate with a pK_a of approximately 4.6. We therefore conclude that the pH dependence of K39 $^{15}\text{NH}_3^+$ chemical shift suggests that it is sensitive to the protonation of a carboxylate, possibly E35, but the other five lysines show no evidence of any interaction with carboxylates.

The HISQC spectra also showed the appearance of a species with four isotope peaks as the titration to low pH progressed (Supporting Information). Such a signal can only be due to NH_4^+ ions present in the sample, which (based on the pK_a of ammonia) are expected to have a faster exchange rate than lysines at higher pH and hence disappear more rapidly as the pH is raised. This assignment was confirmed by buffer exchange.

Deuterium Isotope Effects. Two different deuterium isotope effects can be measured from the HISQC spectra acquired in $\text{H}_2\text{O}/\text{D}_2\text{O}$ mixtures: a $^1\Delta\text{N(D)}$ shift on ^{15}N due to substitution of an attached proton by deuterium, and a $^2\Delta\text{H(D)}$ shift on ^1H due to one of the other protons on the same nitrogen being replaced by deuterium ($^n\Delta\text{X(D)} = \delta\text{X(H)} - \delta\text{X(D)}$ is the n -bond deuterium effect observed on nucleus X). In principle the effect can differ from NH_3^+ to NH_2D^+ and NH_2D^+ to NHD_2^+ , but the difference is expected to be small and is not measurable in our spectra, in agreement with previous studies.²¹ We therefore report an average effect in Table 1.

It is obvious that all the $^1\Delta\text{N(D)}$ values are very similar. By contrast, in model systems there is considerable variation in $^1\Delta\text{N(D)}$: for example, in complexes of ammonium ions with crown ethers, $^1\Delta\text{N(D)}$ varied between 0.277 and 0.364 ppm,²³ with the smaller values found for the complexes that have the closest approach of the crown ether to the ammonium ion. We therefore carried out density functional theory (DFT) calculations for $^1\Delta\text{N(D)}$. The results are shown in Table 2.

It can be seen from Table 2 that replacement of H1 (i.e., the proton directly involved in an $\text{H}\cdots\text{O}$ hydrogen bond) by D results in an isotope effect that is substantially different in a hydrogen-bonded system, with the difference becoming greater as the $\text{N}\cdots\text{O}$ distance shortens. Deuteration of the other protons produces a smaller difference but in the opposite direction. The net result is a decrease of the mean $^1\Delta\text{N(D)}$ as the $\text{N}\cdots\text{O}$ distance is decreased.

Thus, both model compounds and DFT calculations suggest that a direct hydrogen-bonding interaction should lead to significant variation in $^1\Delta\text{N(D)}$. The lack of such an observed effect here is powerful evidence for the absence of any such interaction. The observed values of the deuterium isotope effects are consistent with general solvation.

Further confirmation of this conclusion comes from measurement of isotope effects as the pH is varied. One would expect that deuterium isotope effects would change as a salt-bridged carboxylate becomes protonated. The change in isotope effects with pH is shown in Figure 4. The most obvious trend is a gradual increase in $^1\Delta\text{N(D)}$ as the pH decreases and a decrease in the magnitude of $^2\Delta\text{H(D)}$. This can be ascribed to the addition of HCl to adjust the pH. Chloride ions are known to lead to slightly different isotope effects as compared to the harder ions such as carboxylic acids.²² Otherwise, the only obvious pH-dependent change in deuterium isotope effect is seen for $^2\Delta\text{H(D)}$ of K12, which apparently becomes smaller in magnitude at higher pH. However, this signal is clearly broadened by exchange, and both the line width and apparent isotope effect vary with pH in a manner consistent with pH-dependent exchange broadening. Therefore, the effect seen for K12 is not a real change in isotope effect. We can conclude that there is no clear change in isotope effect (particularly of the more diagnostic $^1\Delta\text{N(D)}$) on protonation of carboxylate side chains.

Rotational Mobility of the $\text{C}_\epsilon\text{--N}_\zeta$ Bond. Recent observations of the J -coupled ^{15}N line shape for lysines in proteins^{29,30} have shown that the intensities of the $^{15}\text{NH}_3^+$ lines in the quartet provide information on the mobility of the $\text{C}_\epsilon\text{--N}_\zeta$ bond. Thus, a rapidly rotating isolated lysine side chain has signal intensities approximately 2.7:1:1:2.7,³⁰ roughly in line with the “methyl-TROSY” effect studied by Kay and co-workers,³⁹ whereas lysines in buried positions in proteins have intensity ratios as different as 0.5:1:1:0.5 for a buried and extensively hydrogen-bonded side chain.³⁰ An HISQC spectrum with no decoupling during t_1 was therefore acquired. ^{15}N quartets were resolved for five of the six residues, the peaks from K39 being too broad to allow all four to be resolved, and are shown in Figure 5. The peak intensities are in an approximate ratio of 1:1.2:1.2:1 for each of the five quartets, which is consistent with the intensities seen in other studies,^{29,30} considering that this study was conducted at a lower temperature than those, where the viscosity of water is considerably greater. The ratio of peak intensities in each quartet is therefore similar for all lysines, and close to the value expected for a freely rotating side chain under these conditions.

Aspartate and Glutamate Side Chain pK_a Determination. The pK_a s of aspartate and glutamate side chains are expected to be lowered by involvement in salt bridges, changes of 0.2–4.0 pH units being found depending on the strength of the interaction. Protein G B1 domain carboxylate pK_a s have been determined previously³³ via observation of proton chemical shift changes. However, it has been shown that changes in the chemical shifts of side chain carbon atoms allow more accurate determination of pK_a s than those of protons,⁴⁰ implying that the published

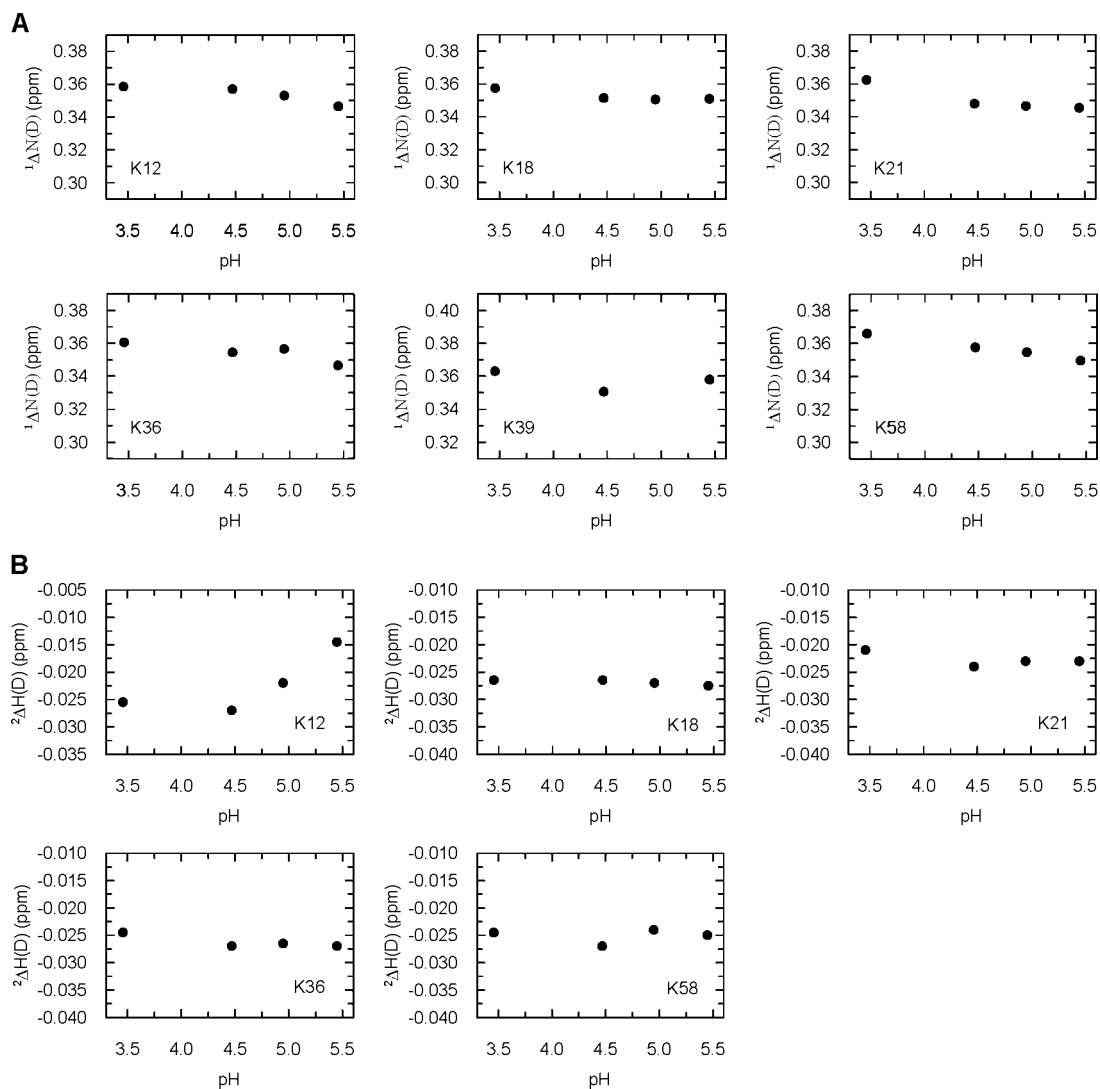


Figure 4. pH dependence of (A) $^1\Delta N(D)$ and (B) $^2\Delta H(D)$. The $^2\Delta H(D)$ for K39 could not be measured because of exchange.

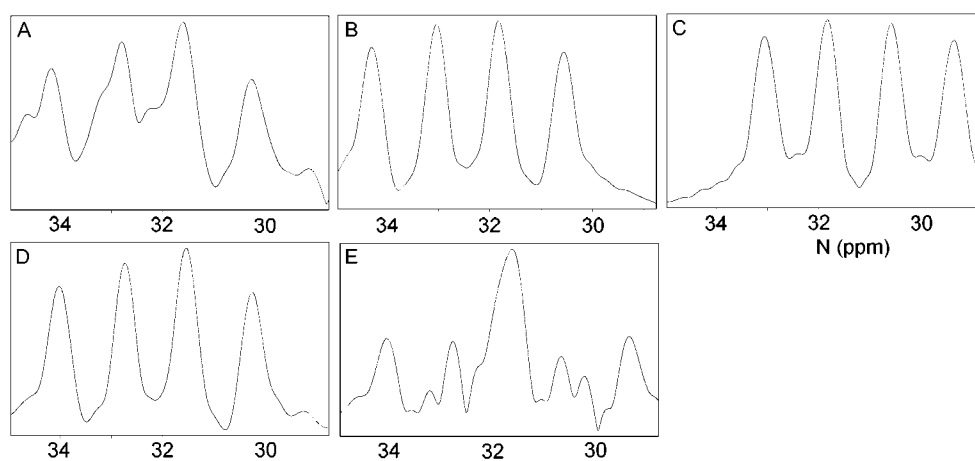


Figure 5. Cross-sections through the J -coupled ^{15}N quartet of lysines (A) K12, (B) K18, (C) K21, (D) K36, and (E) K58 from a coupled HISQC spectrum, pH 5.59, 278 K, 50 mM phosphate in 100% H_2O with a capillary tube of D_2O in the center of the sample. The cross-section for the K58 quartet is not as clear as the remaining four, as these peaks are close in the ^1H dimension to those of K21, and one of the K21 peaks overlaps the K58 quartet, producing a large peak close to the third peak of K58.

values may need re-evaluation. The $\text{p}K_{\text{a}}$ s of aspartate and glutamate side chains were therefore redetermined using changes in side chain carbon and proton chemical shifts with pH, and

10 of the 11 carboxylate side chain $\text{p}K_{\text{a}}$ s were determined, the signals for E50 being too broad and overlapped for reliable fitting.

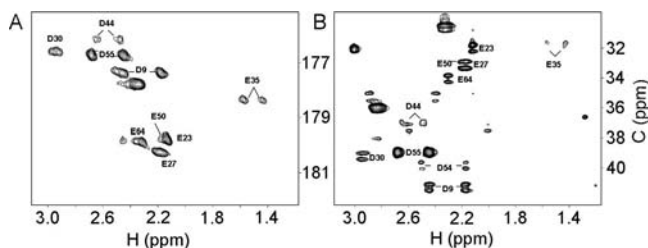


Figure 6. (A) H(C)CO spectrum showing correlations between carboxylate $H\beta/\gamma$ and C' and (B) HC(CO) spectrum showing correlations between the $H\beta/\gamma$ and $C\beta/\gamma$ of carboxylate side chains. Peaks in (B) are doublets due to incompletely suppressed carbon–carbon coupling. No peak for D54 was observed in (A), and peaks for D48 are not visible in (B) but can be observed at lower contour levels.

Table 3. pK_a Values of Aspartate and Glutamate Side Chains in Protein G

residue	pK_a	pK_a determined previously ³³
E23	4.37 \pm 0.01	4.4 \pm 0.1
E27	4.16 \pm 0.01	3.7 \pm 0.15
D30	2.78 \pm 0.01	2.9 \pm 0.1
E35	4.56 \pm 0.04 ^a	4.5 \pm 0.1
D44	3.75 \pm 0.01	3.8 \pm 0.1
D48	4.03 \pm 0.01	4.0 \pm 0.2
E50	— ^b	4.4 \pm 0.1
D54	3.93 \pm 0.01 ^c	3.6 \pm 0.1
D55	3.24 \pm 0.01	3.4 \pm 0.3
E64	3.23 \pm 0.03 and 4.51 \pm 0.04	4.0 \pm 0.1

^a With a Hill coefficient of 0.84. For all other residues the Hill coefficient was 1.0. ^b Not determined as the peak became broad and overlapped at low pH and could not be measured accurately. ^c Determined using $C\beta$ and $H\beta$ chemical shifts only, as the carbonyl peak was not resolved in the H(C)CO spectra.

2D H(C)CO and HC(CO) spectra showing correlations between the $H\beta/\gamma/C'$ and the $H\beta/\gamma/C\beta/\gamma$ respectively were collected every 0.25 pH unit from pH 2.0 to 6.0 and every 0.5 pH unit from pH 6.0 to 9.0. An example of these spectra is shown in Figure 6. The side chain C' , $C\beta/\gamma$, and $H\beta/\gamma$ chemical shift changes with pH for each residue were fitted simultaneously to a single pK_a using eq 1 (Figure 7). All residues fitted well except for E35 and E64 (Figure 7); however, good fits for both residues could be obtained by fitting either to two pK_a s (eq 2), or to a single pK_a but a Hill coefficient different from unity (eq 3). Statistically, either fit was equally good, but by eye, E35 fits better to a single pK_a but a Hill coefficient different from unity, while E64 fits better to two pK_a s (Supporting Information), as listed in Table 3. The latter is expected, because E64 is the C-terminal residue, and chemical shifts are likely to be affected by the titration of the C terminus in addition to the carboxylate side chain. There are no other carboxylate side chains close to E35, and so there is no reason why it should titrate with two pK_a s in this range. A Hill coefficient different from unity is the behavior expected for a charged side chain that has significant interactions with another charged side chain,¹⁹ and our data therefore suggest that E35 may be interacting with another charged side chain. The pK_a s of most of the remaining carboxylate side chains agree well with previously published values,³³ except for E27. They also agree reasonably well with the pK_a s of a mutant of the protein G B1 domain that was determined⁴¹ using carbon chemical shifts.

Comparison of the pK_a s of each carboxylate (Table 3) shows that the pK_a s of carboxylates expected to be involved in salt bridges (E23, E35, and D55) are not generally lower than those of model compounds (3.9 for aspartate and 4.4 for glutamate).⁴⁰ The pK_a of D55 is lower than expected, but this may be due to the proximity of the D54 side chain. The pK_a of D30 is low because it is at the N-terminal end of an α -helix.⁴⁰ In conclusion, the pK_a s of the carboxylate side chains are not noticeably perturbed by any involvement in a salt bridge.

Lysine Side Chain pK_a Determination. The pK_a of a lysine side chain involved in a salt bridge is expected to be higher than the average pK_a of a lysine, as the interaction would favor the positively charged, protonated state. The pK_a s of lysine residues have been less frequently studied than those of aspartates and glutamates due to the difficulty of observing lysine side chain chemical shifts because of rapid hydrogen exchange of the $H\zeta$ and the requirement for proteins to remain stable at high pH. This can lead to incomplete titration curves, adding error to the derived pK_a . Measurement of pK_a using the $C\delta$ chemical shift⁴² is difficult in protein G because of chemical shift overlap, so lysine pK_a s were determined by observation of $N\zeta$ chemical shifts,³¹ which provided more dispersion between the peaks and allows the observation of chemical shifts closer to the protonation site.

Therefore, the pK_a s of the lysine residues in protein G were determined from the change in $N\zeta$ chemical shift with pH. H₂CN spectra were acquired as described,³¹ every 0.5 pH unit from pH 8.0 to 11.0. An example of these spectra is shown in Figure 8. The titration could not be continued past pH 11.0, as the protein unfolded above pH 11.0. The $N\zeta$ chemical shift was plotted against pH for each residue, and the data were fit to eq 1. As the residues had not reached the end of the titration by pH 11.0, the total chemical shift change with pH was fixed to 8.0 ppm to assist the fitting, the figure of 8.0 being derived from previous work.³¹ The lysine side chains have pK_a s ranging from 10.7 to 11.4, as shown in Figure 9 and summarized in Table 4. A fluorescence titration shows that the protein unfolds at approximately pH 11.25, and that at pH 11.0, it is approximately 25% unfolded (Supporting Information). The derived pK_a values could therefore be affected by pH-dependent unfolding. However, a fitting omitting the data at pH 11.0 gave pK_a values identical to within 0.04 pH unit, implying that the error from this source is small.

The pK_a s of the lysine residues do not show evidence for the existence of salt bridges, which would be expected to raise the pK_a s of K12, K39, and K58. The highest pK_a s are those of K21 (which is not expected to form a salt bridge) and K58, while the lowest is that of K12 (which is expected to be involved in a salt bridge). The two highest pK_a s of residues involved in salt bridges are equal to those of two residues that do not form salt bridges, showing that the pK_a s of the salt-bridged lysines are no different than those of the lysines that do not form salt bridges in crystals.

Effect of Buffer Concentration. The experiments described so far, with the exception of the pH titrations, were carried out in 50 mM potassium phosphate at pH 5.5. Under these conditions, there is very little evidence for salt bridges, although differential chemical exchange rates are observed. Both salt bridges and exchange are likely to be affected by the concentra-

(40) Forsyth, W. R.; Antosiewicz, J. M.; Robertson, A. D. *Proteins: Struct., Funct. Genet.* **2002**, *48*, 388–403.

(41) Lindman, S.; Linse, S.; Mulder, F. A. A.; André, I. *Biophys. J.* **2007**, *92*, 257–266.

(42) Gao, G. H.; Prasad, R.; Ludwig, S. N.; Unkefer, C. J.; Beard, W. A.; Wilson, S. H.; London, R. E. *J. Am. Chem. Soc.* **2006**, *128*, 8104–8105.

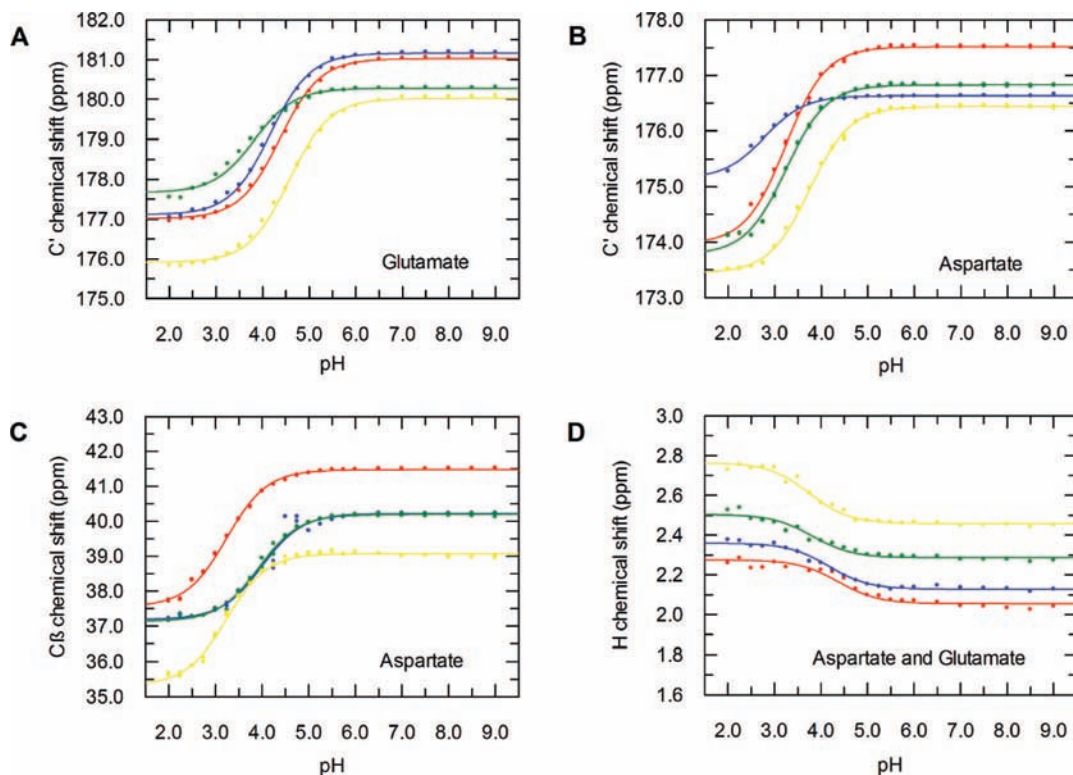


Figure 7. Change in aspartate and glutamate chemical shifts with pH fitted to eq 1. D48 and D54 could not be assigned clearly in H(C)CO spectra due to overlapping peaks, so the pK_a was determined using only data from HC(CO) spectra. (A) Fits of C' shifts for E23 (red), E27 (blue), E35 (yellow), and E64 (green). The fits for E35 and E64 fit sufficiently poorly to imply that the shift is influenced by more than one pK_a . (B) Fits of C' shifts for D9 (red), D30 (blue), D44 (yellow), and D55 (green). (C) Fits of $C\beta$ shifts for D9 (red), D48 (blue), D54 (green), and D55 (yellow). (D) Fits of H shifts for E23 (red), E27 (blue), D44 (yellow), and E64 (green).

tion and composition of the buffer. We have therefore studied the effect of buffer composition.

At lower concentrations of phosphate (Figure 10A), the signals for K39 and K58 are significantly broader (the signal for K12 is obscured), but there is no obvious effect on the other three lysines, which remain sharp. An increase in the concentration of acetate has an effect similar to that of an increase in the concentration of phosphate, in that K39 and K58 become sharper (Figure 10C). However, a higher concentration of acetate is required for the same effect: an increase of 100 mM acetate has an effect on line width similar to that of an increase of 40 mM phosphate.

Discussion

In this work, we have carried out a detailed study of the six lysines of the B1 domain of protein G, to investigate whether the experimental evidence supports the involvement of lysines in salt bridge interactions with aspartates and glutamates. Crystal structures suggest that three of the lysines form salt bridges (K12, K39, and K58), while the other three do not. In no case do we find strong evidence of salt bridges, although there is evidence suggesting that the three “salt bridge” residues are on average closer to carboxylates than are the other three. We discuss briefly each of the experimental measurements.

The chemical shifts of the lysine NH_3^+ groups are similar. The only significantly shifted signal is that for K39, where the 1H shift is approximately 0.4 ppm upfield from the rest. Chemical shift calculations⁴³ show that this is most likely due

to a ring current effect from W51. There is thus no obvious effect of salt bridges on lysine side chain chemical shifts. By contrast, both $^{15}N^{44}$ and 1H shifts⁴⁵ are highly sensitive to structural effects in proteins. The lack of chemical shift change with different buffer composition (Figure 10) further implies that there are no electrostatic effects on ^{15}N or 1H shifts. In addition, the NH_3^+ group proton chemical shifts of all six residues show no change in response to the protonation of the carboxylate side chains. The $N\zeta$ chemical shift of K21 shows a change in chemical shift with pH, but K21 is not involved in any salt bridge interaction. K39 $N\zeta$ chemical shift also titrates, with a pK_a reasonably close to that of its potential salt bridge partner E35. The change in shift is approximately 0.2 ppm. By contrast, very large pH-dependent changes in amide proton and nitrogen chemical shifts are observed in residues with amides that have hydrogen bonds with carboxylate side chains.^{33,46–49}

We also note that the two $C\epsilon H$ protons on each of the six lysines are equivalent, except for those of K39, which differ by 0.30 ppm at pH 7 and 0.25 ppm at pH 11, the pK_a of K39. It therefore appears that chemical shift values for K39 suggest that the amino group senses the presence of a neighboring carboxylate, though the effects are not large enough to imply that a full hydrogen-bonding interaction is present.

(44) Xu, X. P.; Case, D. A. *Biopolymers* **2002**, *65*, 408–423.

(45) Asakura, T.; Taoka, K.; Demura, M.; Williamson, M. P. *J. Biomol. NMR* **1995**, *6*, 227–236.

(46) Bundi, A.; Wüthrich, K. *Biopolymers* **1979**, *18*, 299–311.

(47) Ebina, S.; Wüthrich, K. *J. Mol. Biol.* **1984**, *179*, 283–288.

(48) Szyperski, T.; Antuch, W.; Schick, M.; Betz, A.; Stone, S. R.; Wüthrich, K. *Biochemistry* **1994**, *33*, 9303–9310.

(49) Betz, M.; Löhr, F.; Wienk, H.; Rüterjans, H. *Biochemistry* **2004**, *43*, 5820–5831.

(43) Williamson, M. P.; Asakura, T. *J. Magn. Reson. Ser. B* **1993**, *101*, 63–71.

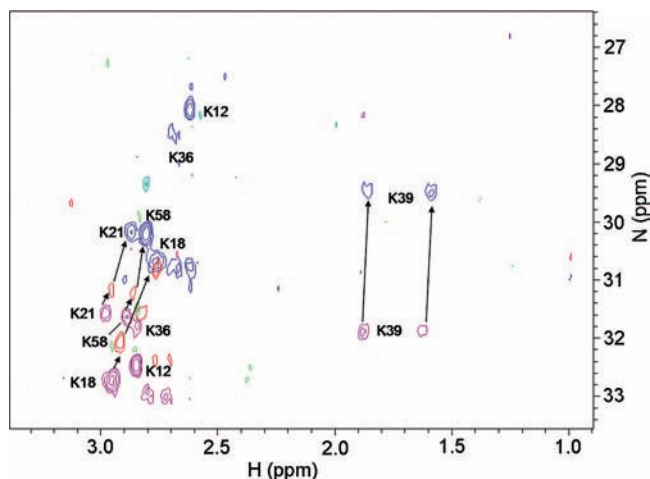


Figure 8. Overlay of H₂CN spectra of lysine NH₃ groups at pH 8.0 (purple), 10.0 (red), and 10.75 (blue).

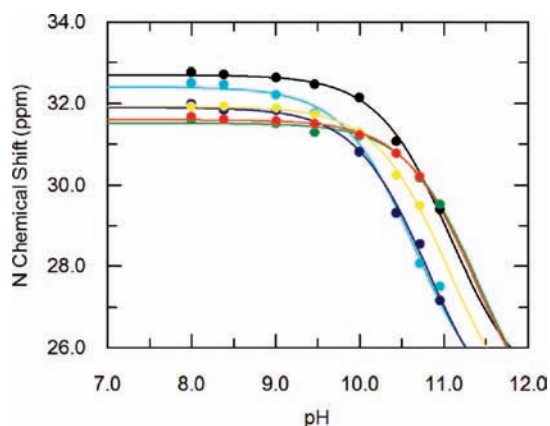


Figure 9. Change in lysine N ζ chemical shift with pH fit to eq 1 for K12 (cyan), K18 (black), K21 (green), K36 (blue), K39 (yellow), and K58 (red).

Table 4. pK_a Values of Lysine Residues in Protein G

residue	pK _a	salt bridge in crystal structure
K12	10.7 ± 0.04	yes
K18	11.1 ± 0.05	no
K21	11.4 ± 0.06	no
K36	10.8 ± 0.04	no
K39	11.1 ± 0.04	yes
K58	11.4 ± 0.08	yes

There is substantial evidence, both experimental and theoretical, that deuterium isotope effects, particularly $^1\Delta N(D)$, differ when the amine is hydrogen-bonded. However, here there is no trend observable in either $^1\Delta N(D)$ or $^2\Delta H(D)$, and no change in isotope effect as the carboxylates are titrated, or with buffer concentration (Figure 10). This is additional strong evidence against any hydrogen bond.

The fact that no difference was seen between the ^{15}N J -coupled quartet intensities shows that there is no evidence of conformational restriction for any of the lysines, as would be expected if the salt bridge was a significant interaction.

Involvement in a salt bridge would be expected to influence the pK_a of both lysine and carboxylate side chains. As the lysine side chain pK_as are not elevated and the carboxylate side chain pK_as are not reduced for those residues involved in salt bridges in the crystal structure, the pK_as provide no evidence for the

existence of the salt bridges in solution. This implies that the solvent-exposed salt bridge is too weak an interaction to affect the pK_as of the side chains involved, unlike buried salt bridges and hydrogen-bonding interactions that do influence the pK_as of the titrating side chains.^{40,50–52} There is a large body of work that relates the change in pK_a to a free energy of interaction.^{1,17,18,20} The fact that there is no observable effect on pK_a may therefore be taken as good evidence that the free energy of interaction between amino and carboxylate groups for all the lysines in protein G in water is small or positive: in other words, that even though in crystal structures the side chains are close together and positioned so as to show a favorable interaction, in solution the favorable enthalpic interaction is outweighed by the unfavorable entropic cost of keeping the two groups together.

Although pK_a values are not noticeably perturbed as described above, fitting of the pK_a of E35 required a Hill coefficient different from unity, implying that E35 may be involved in interactions with another charged side chain. Taken together with the pH-dependent ^{15}N shift of K39 and the nonequivalence of K39 H ϵ protons noted above, it therefore seems likely that the chemical shifts of E35 and K39 side chains sense a mutual interaction, though not one strong enough to affect their pK_a, deuterium isotope effect, or side chain mobility. We therefore conclude that E35 and K39 probably interact for some fraction of the time, i.e., that the free energy for the interaction in water is close to zero. Whether this constitutes a “weak hydrogen bond” or not is a matter of semantics. We note that this interaction is an ($i,i+4$) interaction within a helix, which are well known as interactions that stabilize a helix against unfolding.⁵³ (However, as noted in the Introduction, this observation does not prove that ($i,i+4$) interactions occur in helices. It could also be that such interactions are unfavorable in random coils.)

We have here provided powerful evidence that salt bridges are not present in protein G in solution in 50 mM phosphate buffer (except probably transiently for E35/K39), despite the fact that they are consistently present in crystal structures. This difference is not due to the crystal data being collected at low temperatures, since three of the six structures were obtained at room temperature; moreover, very few changes in hydrogen-bonding are typically seen in crystal structures with temperature.⁵⁴ The difference is all the more remarkable because the crystal structures were collected at high ionic strength, where hydrogen-bonding interactions should be reduced. As noted in the Introduction, experimental studies suggest that exposed salt bridges confer little if any stabilizing energy to proteins. Molecular dynamics simulations in explicit solvent suggest that salt bridges may confer *kinetic* stability, but it is difficult to obtain reliable calculations of free energy from them.⁵⁵ We therefore tentatively suggest that the observations of salt bridges in crystals reflect the need for ordered crystalline arrays as well as a more ordered protein surface caused by the close packing

(50) Laurents, D. V.; Huyghues-Despointes, B. M. P.; Bruix, M.; Thurlkill, R. L.; Schell, D.; Newsom, S.; Grimsley, G. R.; Shaw, K. L.; Treviño, S.; Rico, M.; Briggs, J. M.; Antosiewicz, J. M.; Scholtz, J. M.; Pace, C. N. *J. Mol. Biol.* **2003**, *325*, 1077–1092.

(51) Li, H.; Robertson, A. D.; Jensen, J. H. *Proteins: Struct., Funct. Bioinf.* **2004**, *55*, 689–704.

(52) Thurlkill, R. L.; Grimsley, G. R.; Scholtz, M.; Pace, C. N. *J. Mol. Biol.* **2006**, *362*, 594–604.

(53) Marqusee, S.; Baldwin, R. L. *Proc. Natl Acad. Sci. U.S.A.* **1987**, *84*, 8898–8902.

(54) Tilton, R. F.; Dewan, J. C.; Petsko, G. A. *Biochemistry* **1992**, *31*, 2469–2481.

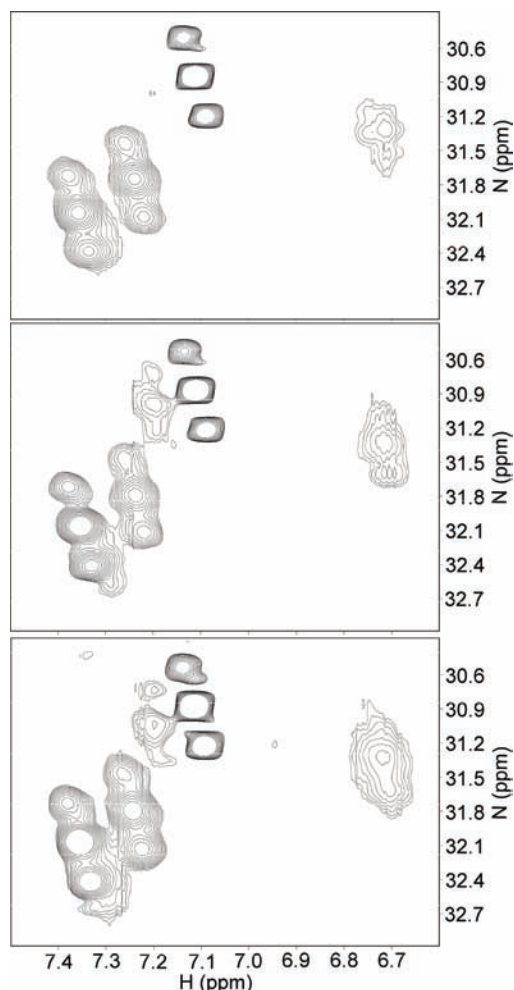


Figure 10. HISQC spectra of protein G, pH 5.7 ± 0.02 , 278 K in 40% D_2O , in (A, top) 10 mM potassium phosphate, (B, middle) 50 mM potassium phosphate, and (C, bottom) 10 mM potassium phosphate plus 100 mM sodium acetate. All spectra were processed identically and are plotted at the same contour levels.

of neighboring molecules, and that the difference seen here between solution and crystal is real.

The most striking difference between K12, K39, and K58 and the other three lysines is their line shapes. These three lysines have broader lines arising from chemical exchange of the amino protons with water. In most of the crystal structures of protein G in the Protein Data Bank,⁵⁶ namely 1pga, 1pgb,²⁸ 2qmt,³⁶ 1mi0,³⁷ 2on8, and 2onq,³⁸ these three residues form salt bridges with carboxylates (Figure 2). Based on previous studies^{29,30} that found residues involved in salt bridges to have slower exchange rates and therefore sharper peaks, this result was initially surprising. The analysis above identifies an exchange rate of approximately 25 s^{-1} for K39, followed by K12 and K58, with the others being slower. Comparison with related data^{57,58} implies an expected intrinsic exchange rate for exposed lysines of around $5\text{--}10 \text{ s}^{-1}$ under our conditions. It is

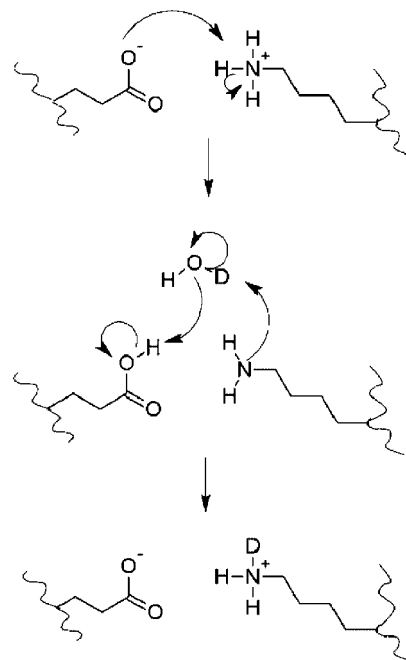


Figure 11. General-base-catalyzed exchange that increases the proton/deuterium exchange rate for lysine NH_3^+ groups from K12, K39, and K58.

therefore likely that K12, K39, and K58 have an accelerated exchange rate rather than K18, K21, and K36 having a reduced exchange rate. The increased exchange rate most likely arises from general-base-catalyzed exchange by the neighboring carboxylates (Figure 11). In support of this argument, we observe that glutamate is observed here to be a more effective general base than aspartate (i.e., exchange of K58 is slower than that of K39 and K12), in agreement with the general observation that the stronger base is usually the better catalyst. This conclusion is supported by the marked broadening of K58 at low ionic strength (Figure 10A).

Buffer composition is expected to have two effects on exchange rates. First, increased ionic strength leads to shielding of charges. A calculation using the extended Debye–Hückel theory,⁵⁹ assuming a small fraction of charge–charge interaction in solution, suggests that 100 mM phosphate should approximately halve the population at pH 5.5, while 100 mM acetate will have a smaller effect because it is less ionized (Supporting Information). If the charge–charge interaction takes the form of a salt bridge, then addition of 100 mM buffer should therefore reduce its population by approximately 50%. No effects on chemical shift or deuterium isotope effect were observed here (Figure 10), further supporting our conclusions that there is no significant population of salt bridge present. On the other hand, if the interaction is sufficient to lead to base-catalyzed exchange but not salt bridge formation, then addition of buffer will reduce the exchange rate and produce sharper signals. This is the observation (Figure 10), implying that K39 and K58, and probably also K12, are broadened by exchange that is catalyzed by the adjacent carboxylate. The reduction in line width is greater from phosphate than from acetate at the same concentration, as expected because of its higher degree of ionization. There is therefore a significant effect from the buffer, which is one of disrupting the interactions that lead to exchange rather than disrupting salt bridges.

(55) Gruia, A. D.; Fischer, S.; Smith, J. C. *Proteins: Struct., Funct. Genet.* **2003**, *50*, 507–515.

(56) Berman, H. M.; Westbrook, J.; Feng, Z.; Gilliland, G.; Bhat, T. N.; Weissig, H.; Shindyalov, I. N.; Bourne, P. E. *Nucleic Acids Res.* **2000**, *28*, 235–242.

(57) Segawa, T.; Kateb, F.; Duma, L.; Bodenhausen, G.; Pelulessy, P. *ChemBioChem* **2008**, *9*, 537–542.

(58) Liepinsh, E.; Otting, G. *Magn. Reson. Med.* **1996**, *35*, 30–42.

(59) Atkins, P. W. *Physical Chemistry*, 5th ed.; Oxford University Press: Oxford, UK, 1994.

The second effect of buffer is itself to act as a general base and catalyze exchange. However, the effect is too small to be detected in our spectra, even for phosphate which is a better catalyst of exchange in lysines.⁵⁸

Unlike previous studies into the effect of salt bridges on the free energy of folding, this study focuses solely on the folded state. Disruption of salt bridge interactions by mutation can have additional effects other than those caused by the loss of the charged group, making it difficult for such studies to separate out the effect due to the salt bridge from additional effects.^{1,15} Such studies also assume no salt bridge interactions are present in the unfolded form, and this may not be the case.^{1,60} The present study, focusing solely on the detection of salt bridges in the folded state in solution, suggests that exposed salt bridges are not significant interactions in solution, even though they are found consistently in crystal structures. Previous work

suggests that buried salt bridges should be more favorable, and this is currently under investigation.

Acknowledgment. We thank Marius Clore (NIH, Bethesda MD) for sending pulse programs for HISQC and related spectra, the reviewers for helpful and constructive comments, and the Biotechnology and Biological Sciences Research Council for funding (J.H.T.).

Supporting Information Available: Details of the Debye–Hückel calculation; an HISQC spectrum at pH 3.46; a comparison of regions from CCH-TOCSY, (H)CCENH₃, and H₃NCECD spectra to show how assignment was carried out; fitting of E35 and E64 to two pK_a values and to one pK_a plus a nonunity Hill coefficient; and the fluorescence titration to determine the stability of protein G at high pH. This material is available free of charge via the Internet at <http://pubs.acs.org>.

(60) Robertson, A. D. *Trends Biochem. Sci.* **2002**, 27, 521–526.

JA808223P